International Journal of Adhesion & Adhesives 31 (2011) 104–111

Contents lists available at ScienceDirect

International Journal of Adhesion & Adhesives

journal homepage: www.elsevier.com/locate/ijadhadh

Experimental study on interfacial shear transfer in partially-debonded aluminum/epoxy joint

Lei Zhenkun [a,*], Fu Minrui [a], Yun Hai [b]

[a] State Key Laboratory of Structural Analysis for Industrial Equipment, Department of Engineering Mechanics, Dalian University of Technology, Dalian 116024, China
[b] School of Transportation and Vehicle Engineering, Shandong University of Technology, Zibo 255049, China

ARTICLE INFO

Article history:
Accepted 20 October 2010
Available online 5 November 2010

Keywords:
Load transfer
Interfacial debond
Adhesive joint
Digital photoelasticity

ABSTRACT

A six-step phase-shifting method is applied to calculate the whole-field shear stress of an adhesively bonded aluminum alloy-to-epoxy joint containing an initially debonded interfacial crack for studying shear transfer behavior. For a well-bonded interface, the isochromatic fringe order and the interfacial shear stress (ISS) distribute continuously and increase with compression. The epoxy corner formed at the right-angle edges of the bonded interface during specimen preparation exhibits more than eight orders of dense fringes and a maximum shear stress of 1.4 MPa under a load of 3.0 kg. The load is transferred by a shear band that connects the bonding interface to the support.

A denser isochromatic pattern occurs at the crack-tip than at the right-angle edge from the partially debonded interface. The crack-tip displays about seven fringe orders, 1.3 MPa of ISS under a load of 3.0 kg, and an increase of about 3 mm in the interfacial crack length. The shear stress decreases rapidly at the debonded interface but takes 26% of the shear force of the entire interface, indicating that the debonded interface obstructs and decreases the load transfer capability from the bonding interface to the support.

As the curing temperature decreases to 20 °C, a thermal residual shear stress appears on the interface because of the discrepancy in the coefficients of thermal expansion between the aluminum alloy and the epoxy. The residual shear stress redistributes on the bonded and debonded interfaces due to the formation of the initial crack induced by an external load. The calculated effective stress intensity factors (SIFs) of the interface crack are identical to theoretical prediction.

1. Introduction

The adhesive bonding of dissimilar or similar materials is used in numerous primary aircraft structures. Shear failure easily happens to the bonding interface of multilayer and metal-to-polymer joints. The maximum load has interesting correlations with different surface preparation procedures, interface formation, and interface aging conditions [1]. Complex geometry and material properties make the direct measurement of interfacial mechanical property and bonding edge singularity difficult to perform. Numerical simulation, therefore, is a useful tool for the prediction of the failure mode of a given bonding system [2–4].

The discrepancy of thermal mechanical properties at the interface of adhesive bonding structures of different materials can directly induce thermal stresses that are self-balanced [5,6]. Adams' research shows that thermal stresses coupled with the external load influence the mechanical behavior of the adhesive bonding system [7,8]. In a mixed adhesive joint of titanium/composite with a gap on the adhesive interface, the dissimilar adhesive system affects the mechanical properties exhibited under low and high temperature environments. The difference in the coefficients of thermal expansion (CTE) of the specific dissimilar systems is responsible for this thermal effect [9,10]. More importantly, there is a need to study further the effects of interfacial debonding and cracking on the mechanical properties of the bond interface of a partially debonded adhesive joint.

Aside from the standard testing methods like flexure, lap shear, torsion and peel tests [7,8], optical methods such as photoelasticity and the Moiré interferometry have been used to assess the strength, load transfer and edge singularity of an adhesive bonding interface [11,12]. Photoelasticity is the most direct technique to measure interfacial adhesive bonding [13]. A phase-shifting automated polariscope is especially useful in measuring ISS and stress concentration at the fiber-end. The instrument can simultaneously capture four images to produce whole-field maps of isochromatic and isoclinic parameters. The automated polariscope obtains real-time shear stress data in the matrix and at the interface during fiber fracture and interface debonding [14].

Isochromatics and isoclinics, the basic parameters in photoelastic stress analysis, can be obtained by many phase-shifting methods. However, the "uncertain" isoclinic phase map generally includes the first and the second principal stress directions

* Corresponding author. Tel.: +86 411 84708406.
E-mail address: Leizk@163.com (L. Zhenkun).

0143-7496/$ - see front matter © 2010 Elsevier Ltd. All rights reserved.
doi:10.1016/j.ijadhadh.2010.11.003

simultaneously [15,16]. The "uncertain" isoclinic property causes some "ambiguity" to appear in the wrapped phase map of isochromatics and results in an incorrect unwrapping procedure [17,18]. The four-step color phase-shifting method based on a white-light plane polariscope is a more effective process because it needs only four images to determine the principal stress direction with a complicated unwrapping procedure [19]. Based on the four-step color phase-shifting method, a six-step phase-shifting method was proposed to calculate the whole-field shear stress and to avoid the ambiguous isochromatic phase map. The technique was then applied to an aluminum alloy/epoxy joint for studying shear transfer behavior [20].

In this paper, the phase-shifting digital photoelasticity experimental technique was introduced and applied to measure the whole-field shear stress in a heterogeneous adhesive joint of aluminum alloy (AL) and epoxy with a partially debonded interface. To investigate the stress transfer behavior, the maximum shear stress at the interface crack and its crack length was obtained from experimental data. Finally, the effective stress intensity factors of the interface crack were calculated and compared with the theoretical prediction.

2. Digital phase-shifting photoelasticity

Automated stress analysis using photoelasticity requires isochromatic and isoclinic parameters specifically in the first principal stress direction [16]. In this study, the first principal stress direction with an interval $(-\pi/2, \pi/2]$ is defined as the angle of the first principal stress and horizontal reference axis.

2.1. Four-step color phase-shifting method

Fig. 1(a) shows a normal-plane polariscope with rotation angle β, where the polarizer and analyzer are oriented at $\alpha=\pi/2+\beta$ and β from the reference axis x, respectively. The denotations of δ and θ are the phase retardation and the direction of the first principal stress in the model, respectively. When the angle β is synchronously rotated to 0, $\pi/8$, $\pi/4$, and $3\pi/8$, four images are acquired, and a corresponding phase-shifting algorithm is expressed as [19]

$$\theta=\pi/8-0.25\tan^{-1}\left[\frac{J_1-J_3}{J_2-J_4}\right],\quad \text{and}\quad \sin\delta\neq 0. \tag{1}$$

Using white light incidence to reduce the effect of the isochromatic parameter, the intensities in Eq. (1) is equal to the average grey-values of RGB color channels, i.e., $J_i=(J_{ir}+J_{ig}+J_{ib})/3$, $i=1, 2, 3, 4$.

The isoclinic wrapped phase interval $[0, \pi/4]$ can be obtained from Eq. (1) and extended to the wrapped phase interval $[0, \pi/2]$ or $(-\pi/4, \pi/4]$. In fact, the automated determination of isoclinic property is a phase unwrapping process, i.e., converting the wrapped isoclinic phase to the interval $\theta_u\in(-\pi/2, \pi/2]$. The basic concept has been reported in a Ref. [19].

2.2. Improved six-step phase-shifting method

Fig. 1(b) shows a general-circle polariscope. The polarizer and the first-quarter waveplate subtend angles $\pi/2$ and $\pi/4$ to the reference axis x, respectively. The second-quarter waveplate and the analyzer subtend angles γ and β from the reference axis x, respectively. Adapting homochromatic radiation, six images are acquired in different configurations of γ and β, (I_i, $i=1, 2, \ldots, 6$. see details in Ref. [21]), and the six-step phase-shifting algorithm is obtained as

$$\theta=0.5\tan^{-1}\left[\frac{I_5-I_3}{I_4-I_6}\right],\quad \text{and}\quad \sin\delta\neq 0, \tag{2}$$

$$\delta=\tan^{-1}\left[\frac{(I_5-I_3)\sin 2\theta+(I_4-I_6)\cos 2\theta}{I_1-I_2}\right]. \tag{3}$$

The isoclinic phase interval $(-\pi/4, \pi/4]$ and the isochromatic phase interval $[-\pi, \pi]$ can be obtained from Eqs. (2) and (3), respectively. However, the isoclinic phase map obtained from Eq. (2) simultaneously includes the areas of the first and the second principal stress directions. The "uncertain" isoclinic phase causes some "ambiguity" to appear in the wrapped isochromatic phase map using Eq. (3). To avoid this "ambiguity," an unwrapping isoclinic interval $\theta_u\in(-\pi/2, \pi/2]$ was determined and extended by the four-step color phase-shifting method. This was then substituted to the "uncertain" isoclinic phase interval $(-\pi/4, \pi/4]$ in Eq. (3). The equation was transformed to [20]

$$\delta=\tan^{-1}\left[\frac{(I_5-I_3)\sin 2\theta_u+(I_4-I_6)\cos 2\theta_u}{I_1-I_2}\right]. \tag{4}$$

The improved equation avoids the ambiguous isochromatic wrapped phase and is useful in the next unwrapping procedure.

2.3. Automated determination of whole-field shear stress

Using the unwrapped isoclinic phase interval $\theta_u\in(-\pi/2,\pi/2]$ from the four-step color phase-shifting method and the unambiguous wrapped isochromatic phase acquired from the improved six-step phase-shifting method, an unwrapped isochromatic phase, δ_u, is obtained. The whole-field shear stress, τ, can then be conveniently calculated by [22]

$$\tau=\frac{\delta_u f_\sigma}{4\pi h}\sin 2\theta_u, \tag{5}$$

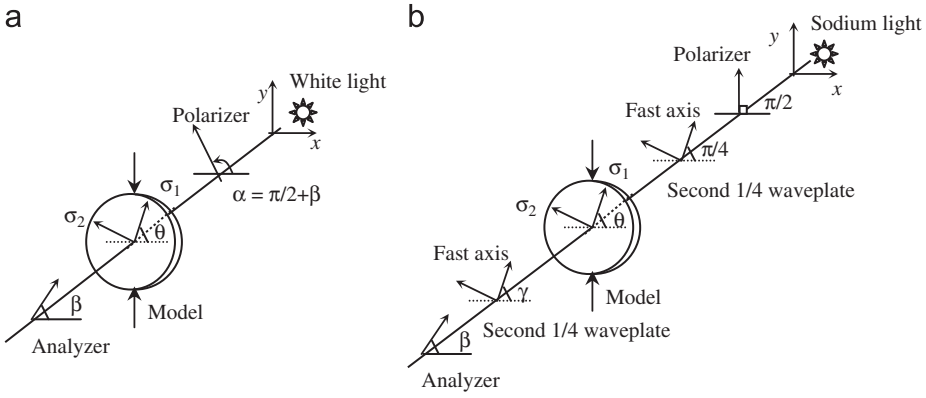

Fig. 1. (a) Normal-plane polariscope at rotation with the angle of β and (b) general-circle polariscope with an arbitrary analyzer and second-quarter waveplate.